

Study of radon removal performance of silver-ion exchanged zeolite from air for underground experiments

T. Sone¹, Y. Takeuchi^{1,2,*}, M. Matsukura³, Y. Nakano⁴, H. Ogawa⁵, H. Sekiya^{6,2}, T. Wakihara^{7,3}, S. Hirano⁸, and A. Taniguchi⁹

¹*Department of Physics, Graduate School of Science, Kobe University, Kobe, Hyogo 657-8501, Japan*

²*Kavli Institute for the Physics and Mathematics of the Universe (WPI), The University of Tokyo Institutes for Advanced Study, University of Tokyo, Kashiwa, Chiba 277-8583, Japan*

³*Institute of Engineering Innovation, School of Engineering, The University of Tokyo, Bunkyo, Tokyo 113-8656, Japan*

⁴*Faculty of Science, University of Toyama, Toyama 930-8555, Japan*

⁵*CST Nihon University, Chiyoda, Tokyo 180-0011, Japan*

⁶*Kamioka Observatory, Institute for Cosmic Ray Research, the University of Tokyo, Gifu 506-1205, Japan*

⁷*Department of Chemical System Engineering, The University of Tokyo, Bunkyo, Tokyo 113-8656, Japan*

⁸*Tosoh Corporation, Chuo, Tokyo 104-8467, Japan*

⁹*Sinanen Zeomic Co., Ltd., Nagoya, Aichi 455-0051, Japan*

.....
Radon is a common background source for underground astroparticle physics experiments and its removal is essential. In this study, we fabricated several prototype silver-ion exchanged zeolites, measured their radon adsorption properties, and evaluated their applicability for radon removal in underground experiments. As a result, we succeeded in producing a prototype silver-ion exchanged zeolite that showed better radon adsorption properties than preceding studies.
.....

Subject Index H20

1. Introduction

Since underground location can greatly reduce the effects of cosmic rays, it is ideal for the astroparticle physics experiments that require extremely low background, such as solar and supernova neutrino observation experiments and direct dark matter search experiments (hereafter referred to as underground experiments). One of the main backgrounds common to underground experiments is the radioactive noble gas radon-222 (hereafter referred to as radon, Rn). For example, the radon concentration in the ambient air near the Super-Kamiokande detector, the world's largest neutrino detector located underground in Kamioka, Japan, ranges from 50 to 2000 Bq/m³ [1, 2], but for accurate solar neutrino observation, the radon concentration in water in the detector must be kept below around 1 mBq/m³. In the

XENONnT experiment, which is a direct search for dark matter in Gran Sasso, Italy, the radon concentration in liquid xenon must be kept below about $4 \mu\text{Bq/kg}$ [3]. Radon removal by activated carbon columns [4, 5] and radon removal by distillation equipment [6] have been developed and operated for reducing radon in these experiments, but both are rather large devices. Due to the high space cost in the underground experimental area, the future planned experiments will require smaller equipment for radon removal.

On the other hand, in industry, zeolite, a crystalline porous material with homogeneous pores of about 0.2 to 1.0 nm, is widely used as an adsorbent, desiccant, ion exchanger, catalyst, wastewater treatment, and so on. Silver-ion exchanged zeolite (Ag-zeolite), in which silver ions are introduced into the zeolite by ion exchange, has also been commercialized as a material with antibacterial and deodorizing properties. There are various types and applications of Ag-zeolites, and various research reports have been done, for example, at the recent conferences held by the Japan Zeolite Association, and/or the Japan Society on Adsorption. An example of a research topic related to this study is the report that Ag-FER (Ferrierite) exhibit excellent separation and adsorption properties for xenon in the atmosphere [7].

In addition, recent studies have reported that Ag-zeolites have very high adsorption performance with respect to radon in air [8, 9]. It is reported that the radon adsorption performance of Ag-ETS-10 (Engelhard Titano-Silicate, a zeolite analog) and Ag-ZSM-5 (zeolite socon Mobil-Five, or Ag-MFI) at room temperature is equivalent to about 500 times that of activated carbon, which could significantly reduce the size of conventional large-scale radon removal systems. Our research group also produced Ag-FER and Ag-MFI in powder form in 2023 and confirmed their ability to adsorb radon in air at room temperature. However, it is also reported in these papers [8, 9] that the adsorption capacity of radon is significantly reduced in high-humidity air. While radon adsorption by granular activated carbon and activated carbon fiber uses physical adsorption due to van-del-Waals forces in the pores, it has been pointed out that the strong adsorption performance of xenon and other noble gases by Ag-zeolite is due to chemical adsorption by silver (metallic silver or silver ions), which has not yet been understood at the molecular level [10]. In any case, if chemical adsorption for radon is possible, radon removal should be much more powerful than the traditional radon removal using physical adsorption in the underground experimental field.

The activated carbons used in underground experiments have reached a level of intrinsic radon emanation in the order of less than 10 mBq/kg [11, 12]. In order to apply Ag-zeolites in underground experiments, the intrinsic radon emanation from the Ag-zeolite should be kept below the similar level. Industrial products are generally not concerned with radon emanation amounts, and the studies in Ref. [8] were done at kBq/m^3 radon concentration levels. Ref. [9] reported a radon emanation of $71 \pm 1 \text{ mBq/kg}$ from Ag-ETS-10, and Ref. [13] reported a radon emanation of $14.2 \pm 7.0 \text{ mBq/kg}$ from 5A zeolite (Ca-Zeolite A) synthesized using low-radioactivity raw materials.

In this study, we focused on the Ag-FER, which was reported to show excellent xenon adsorption performance in air in Ref. [7] and our research group also confirmed its radon adsorption ability in air. We produced new Ag-zeolite samples and measured the radon concentration in air after processing with the Ag-zeolite, the humidity dependence of the radon adsorption performance in air, and the silver introduction dependence of the radon adsorption performance. The results of these measurements are reported in this article.

2. Preparation of Ag-FER zeolites

In this study, samples were prepared from a pellet-shaped ferrielite zeolite HSZ-722HOD1A(H-type) manufactured by Tosoh Corporation, and doped with silver at Sinanen Zeomic Co., Ltd. Table 1 shows the basic properties of the raw material zeolite. The raw

Table 1 Summary of basic properties of raw zeolite made by Tosoh Corporation.

Crystal form	Pore size	Shape	Binder type	Cation	SiO ₂ /Al ₂ O ₃ ratio	Bulk Density
Ferrierite	4.8 Å	1.5 mm ϕ pellet	Alumina	H ⁺	18 mol/mol	0.56 Kg/L

zeolite is in the form of 1.5 mm diameter pellets solidified with alumina binder and has a nominal pore size of 4.8 Angstroms. Table 2 shows the properties of the Ag-zeolite produced in this study. In this study, samples with silver contents of about 3% and about 8% were

Table 2 Summary of basic properties of silver zeolite made by Sinanen Zeomic Co., Ltd.

	Target Silver Amount	Silver introduction process	Measured Silver Amount
3Ag-FER	3%	Normal ion exchange	3.2%
8Ag-FER-D	8%	Impregnation and drying	8.1%
8Ag-FER-B	8%	Special ion exchange	8.4%

produced. The 3% sample was produced by the conventional ion-exchange method, while the 8% samples were produced using two different silver introduction methods.

Figure 1 shows a photograph of the fabricated Ag-zeolite pellets (8Ag-FER-D). To confirm



Fig. 1 Ag-zeolite pellet (8Ag-FER-D) made by Tosoh Corporation and Sinanen Zeomic Co., Ltd.

the distribution of silver inside the pellets, the pellet cross section of silver-exchange zeolite was analyzed by energy dispersive X-ray fluorescence analysis (EDX). Figure 2 shows the results. In all of the prototypes, silver was found to be introduced to the center of the pellet.

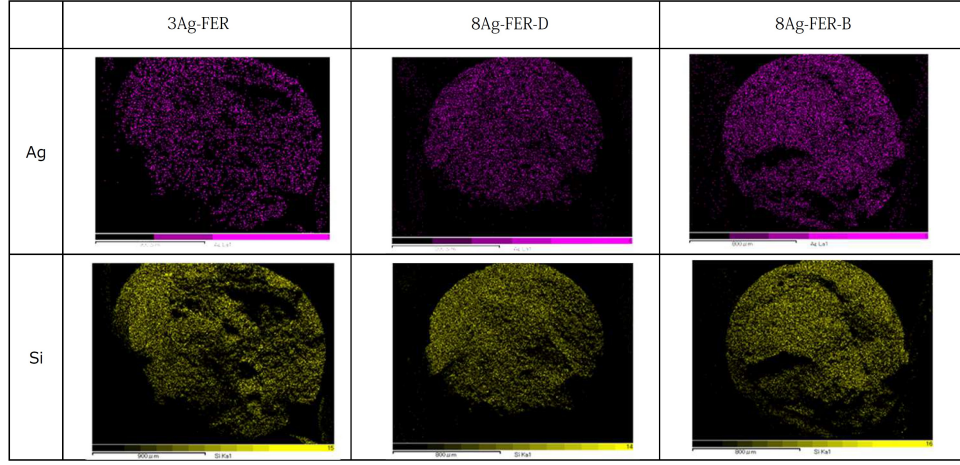


Fig. 2 EDX measurement results of cross section of silver zeolite pellets. The upper panel shows the distribution of silver and the lower panel shows the distribution of silicon.

3. Evaluation system for radon adsorption performance

Figures 3 and 4 show the radon adsorption performance evaluation system developed at Kobe University.

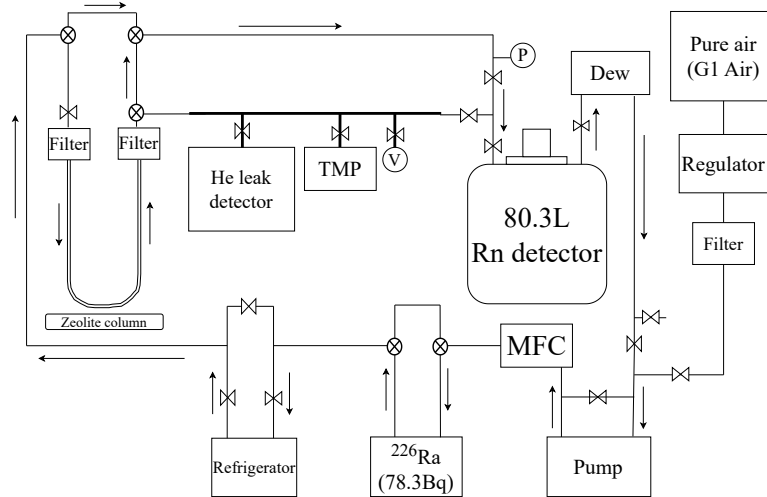


Fig. 3 Experimental setup of the radon adsorption measurement system at Kobe University. P is a pressure gauge, V is a vacuum gauge, and Dew is a dew point gauge.

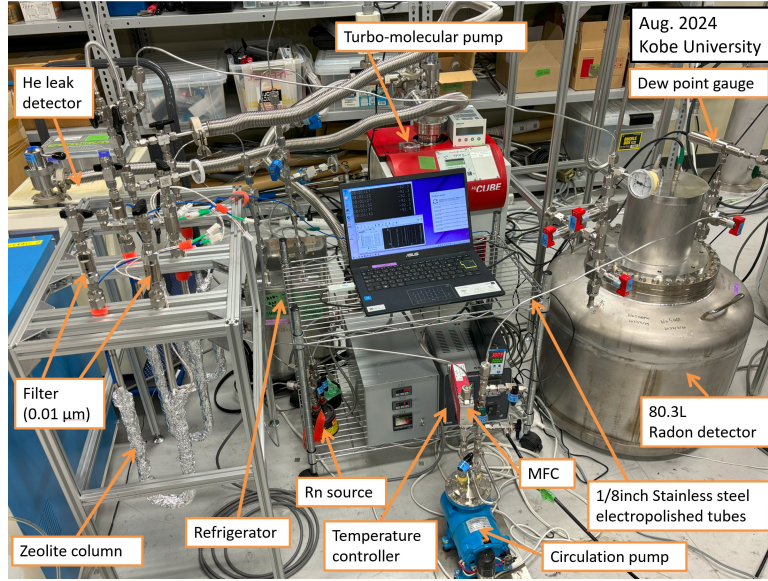


Fig. 4 Photo of the experimental setup at Kobe University.

Various measurements were performed using this apparatus under a room temperature environment of about 21–25°C. The apparatus was filled with pure air (TAIYO NIPPON SANSO G1 Air) at about atmospheric pressure (differential pressure +0.003 to +0.004 MPaG) as a carrier gas. A mass flow controller (MFC, Horiba SEC-Z500X) and a circulation pump (Enomoto Micro Pump MX-808ST-S) were used to circulate the carrier gas through the system at a flow rate of 1.57 to 3.00 L/min. The temperature of the refrigerator (Taisho TC0147) was set at -70°C to -90°C to control the humidity in the system. Humidity in the carrier gas was monitored with a dew point gauge (Vaisala DMT152). A radon source (PYLON RNC, 78.3 Bq at radiative equilibrium) was connected at all times, and the radon concentration in the system was measured with an 80.3 L radon detector with almost the same performance as the 80 L radon detector developed in Refs. [5, 14, 15]. Ag-zeolites were placed in three nearly identical 1/2-inch stainless steel, 1-m-long U-shaped columns. Figure 5 shows a photograph of the U-shaped column used for the measurement using a 20 g sample.

A typical operating procedure is as follows.

- (1) Switched the U-shaped column to bypass, circulated the carrier gas with the radon source connected, and checked the radiative equilibrium curve of radon concentration.
- (2) If switching to the measurement of a different sample, the U-shaped column was replaced and the Ag-zeolite was baked while evacuating with a turbo molecular pump (TMP). The baking was done at 200°C , typically for several hours, and was conducted to an vacuum level of 1×10^{-1} to 1×10^{-3} Pa at 200°C . Evacuation was continued after the heater was turned off, and finally the vacuum in the column reached $4 \sim 8 \times 10^{-4}$ Pa at room temperature. The temperature setting of the refrigerator was also changed at this timing if necessary.
- (3) After the U-shaped column reached room temperature, switched from bypass to via U-shaped column and began radon adsorption measurement.

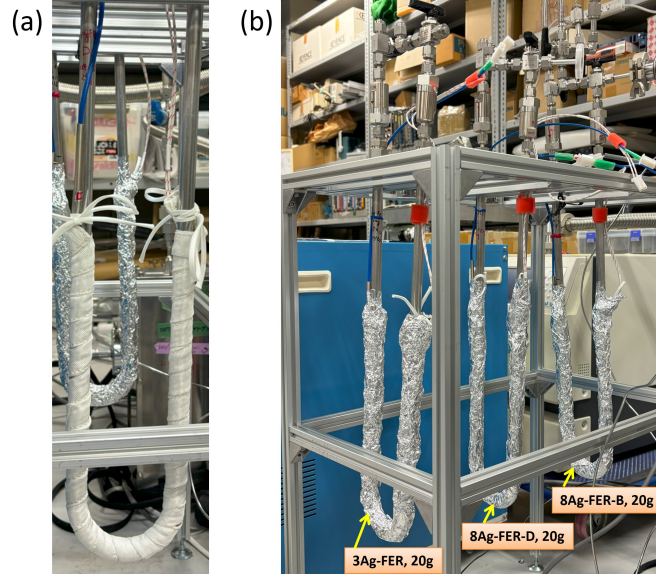


Fig. 5 (a) Typical, U-shaped column with a thermocouple thermometer and 150 W ribbon heater attached. (b) In addition, columns with three types of Ag-zeolite insulated with aluminum foil.

- (4) When the radon concentration became stable, the radon concentration ratio (Rn_{ratio} , see below) was measured. Then, the U-shaped column was baked at 200°C while the carrier gas circulation through the U-shaped column was continued to remove the radon adsorbed in the column. After this, returned to step-(1).

4. Estimation of retention time and radon adsorption coefficient

The time that radon stays in the adsorbent is generally referred to as retention time. In Refs. [8, 9], the performance of radon adsorption is evaluated using the radon adsorption coefficient (K [m^3/kg]), which is defined as

$$K = \frac{F \times RT}{m}, \quad (1)$$

where F [m^3/day] is air flow rate, RT [day] is radon retention time on adsorbent, and m [kg] is mass of adsorbent.

In this study, RT and K were measured and evaluated as follows.

Since the radon sources are always connected, 78.3 Bq of radon is distributed in the system. The radon distribution is assumed to be proportional to the fraction of time when radon stays in each device. The devices with the longest radon stay time in this system are the U-shaped column and the radon detector, and the other devices such as piping are ignored. When the flow rate of the carrier gas is F [m^3/day], the time that radon stays in the radon detector (T [day]) is $T = 0.0803/F$, given the volume of the radon detector (0.0803 m^3). Also, radon should stay in the U-shaped column for the retention time (RT [day]). Therefore, the fraction of radon that stays in the radon detector during circulation through the U-shaped column (called radon concentration ratio: Rn_{ratio}) can be expressed as

$$Rn_{ratio} = \frac{T}{RT + T} = \frac{0.0803}{F \times RT + 0.0803}. \quad (2)$$

On the other hand, the measured value of Rn_{ratio} can be obtained from the ratio of the radon concentration when circulating via the U-shaped column to that when the U-shaped column is bypassed, like

$$Rn_{ratio} = \frac{\text{Rn concentration via column}}{\text{Rn concentration bypassing column}}. \quad (3)$$

Therefore, in this study, the measured radon concentration ratio was obtained when the radon concentration was stable, then RT was obtained from Eq. (2), and then K was evaluated from Eq. (1).

Possible systematic error in this evaluation method is gas flow rate uncertainty (1%). This uncertainty is taken into account in the measurement results in the next section.

5. Results

At first, we filled as much as possible (44 g) of 8Ag-FER-B throughout the 1/2 inch diameter, 1-m long U-shaped column and performed radon adsorption measurements at a flow rate of 1.57 SLM (standard litter per minute) and a refrigerator setting temperature of -90°C . The result is shown in Figure 6. After changing the gas circulation from U-shaped column

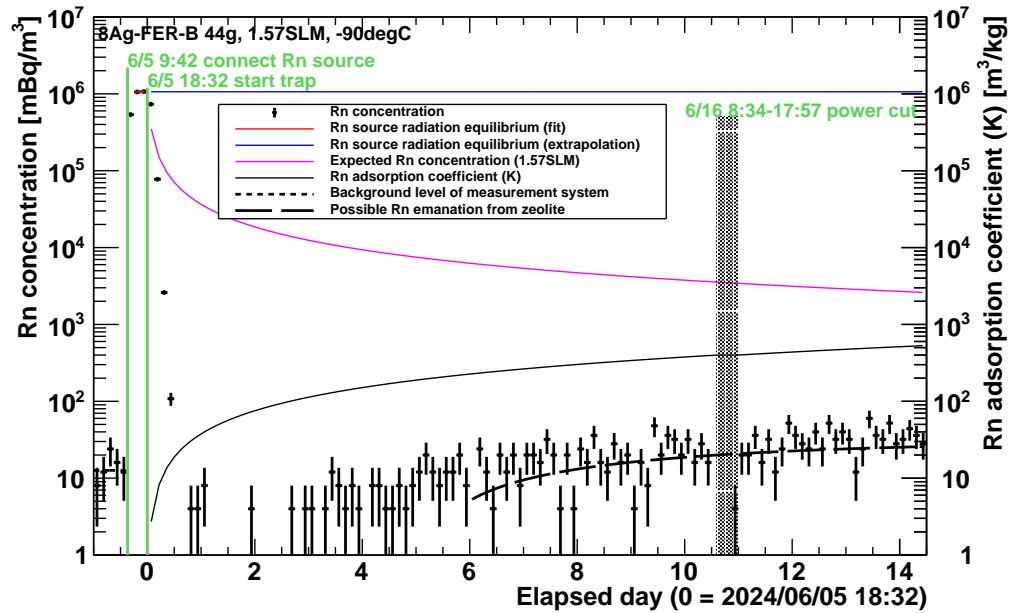


Fig. 6 8Ag-FER-B 44g, 1.57 SLM, -90°C (type and amount of Ag-zeolite, carrier gas flow rate, refrigerator temperature) measurement. Horizontal axis is elapsed day from the U-shaped column connection. The left (right) vertical axis is radon concentration in the radon detector (Rn adsorption coefficient). The hatched area was not available to acquire data due to a planned power cut.

bypass to via U-shaped column, we confirmed that our prototype Ag-zeolite adsorbed radon. Just before connecting the radon source to the system (around Elapsed day = -0.5 days in Figure 6), the background level of the measurement system was at $12.6 \pm 3.2 \text{ mBq/m}^3$. The

radon concentration in the output air was lower than this background level up to around 5 days after the column was connected. After that, a gradual radon leakage was observed, however, it would take several months to measure the retention time (until the measured radon concentration matched the expected radon concentration). Based on the results of this measurement, in order to evaluate the retention time, we took measures to reduce the amount of zeolite (from 44 g to 20 g) and increase the flow rate (from 1.57 SLM to 3.00 SLM) in subsequent measurements. For 3Ag-FER, the humidity dependence of the radon adsorption coefficient was measured at two different refrigerator temperature settings, -70°C and -90°C .

Figure 7 shows an example of a radon adsorption test after the conditions were changed. Figure 7(a) is a plot of the same definition as in Figure 6. Reducing the amount of adsorbent

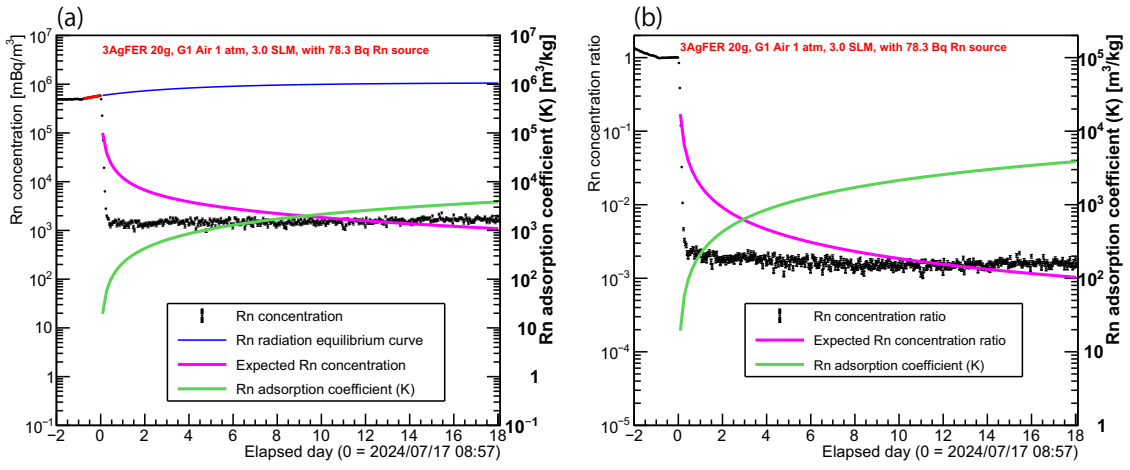


Fig. 7 3Ag-FER 20g, 3.00 SLM, -90°C measurement. (a) Rn concentration. (b) Rn concentration ratio.

and increasing the flow rate enabled stable radon concentration measurements, even via the U-shaped zeolite column.

The data points in Figure 7(b) show the radon concentration ratio from Eq. (3). They were obtained by dividing the measured radon concentration (black dots in Figure 7(a)) by the radiative equilibrium curve with radon source (blue line in Figure 7(a)). The average value of the data points of the radon concentration ratio in Figure 7(b) in the stable region (after Elapsed day = 8 days) is the measured value of the radon concentration ratio. The purple line in Figure 7(b) is the value of the radon concentration ratio obtained by Eq. (2) when the number of elapsed days = retention time, and the elapsed time at the intersection of this curve and the measured value of the radon concentration ratio is the measured value of RT . When the elapsed day = retention time, the green line in Figure 7(a) and (b) shows the K obtained by Eq. (1), and the measured value of K is obtained from the measured value of RT with this function. In this measurement case, we obtained $Rn_{ratio} = 0.0016$, $RT = 12$ days, and $K = 2.6 \times 10^3 \text{ m}^3/\text{kg}$, respectively.

Figure 8 summarizes the results of each measurement in this study where the mass of the adsorbent material was matched to 20 g. The Rn_{ratio} was obtained for each measurement.

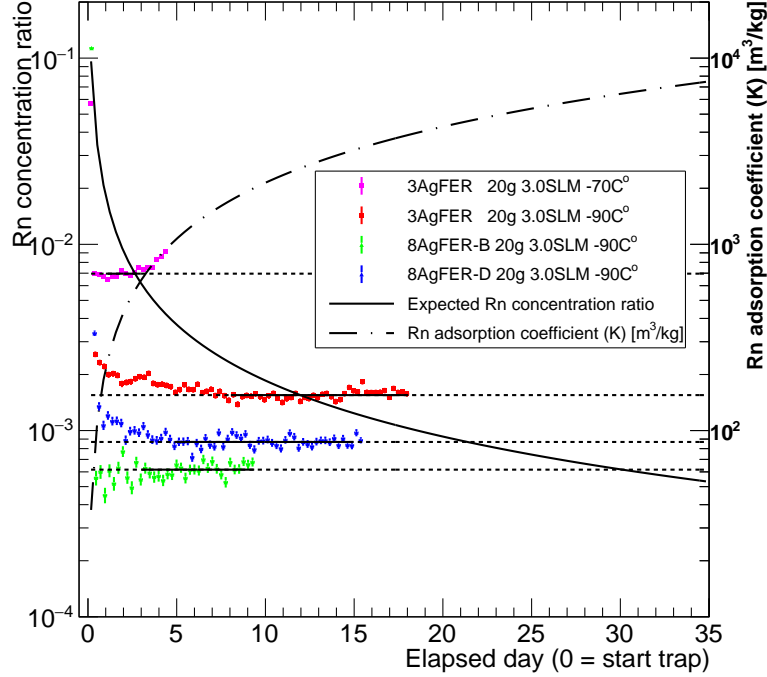


Fig. 8 Measurement results using 20 g of adsorbents. In each measurement data, the horizontal solid line is the measurement period to obtain the Rn_{ratio} value, and the horizontal dotted line is the extrapolation of that line. The elapsed day at the intersection of these horizontal lines and the black curve of the expected radon ratio is the measured value of RT , and the dotted-dashed line at that elapsed day shows the measured value of K .

Periods when Rn_{ratio} was not stable, such as immediately after the start of radon trapping, were excluded from the measurement of mean values. The values of RT and K obtained in this study and those in preceding studies are summarized in Table 3. Interpretations on these data are given in the next section.

6. Discussion

In this section, the obtained results are discussed.

6.1. Radon emanation from Ag-FER

The dashed line in Figure 6 is a fit with the radiative equilibrium function of radon assuming radon emanation in the measurement system containing Ag-zeolite after Elapsed day = 6, yielding the radon concentration at radiative equilibrium to be 31.4 ± 2.9 mBq/m³. Subtracting the background level of 12.6 ± 3.2 mBq/m³ from the measurement system, the radon emanation becomes 18.8 ± 4.3 mBq/m³. Assuming that all of these are emanated from the Ag-zeolite, and considering the amount of the zeolite and the volume of the radon detector, the radon emanation from 8Ag-FER-B becomes 45 mBq/kg at the 90% upper limit. It may emanate less radon than the Ag-zeolite in Ref. [9], but may emanate more radon than the low-radioactivity zeolite in Ref. [13]. This radon emanation level is comparable to

Table 3 Summary of retention time (RT) and radon adsorption coefficient (K). The value with (*) are estimated by us.

Sample	Refrigerator setting	Adsorbent mass [kg]	Retention time [day]	Radon adsorption coefficient [m^3/kg]
(This work)				
3Ag-FER	-70°C	0.020	2.65 ± 0.04	573 ± 4
3Ag-FER	-90°C	0.020	11.97 ± 0.14	2563 ± 14
8Ag-FER-B	-90°C	0.020	30.12 ± 0.48	6506 ± 81
8Ag-FER-D	-90°C	0.020	21.38 ± 0.27	4618 ± 35
(Preceding studies)				
Ag-ZSM-5 [8]		8.85×10^{-3}	10.69	3500
Ag-ETS-10 [8]		16.3×10^{-3}	19.16	3400
Ag-ETS-10(18°C) [9]		2×10^{-4}		$(140 \pm 28) \times 10$
Activated Carbon Fiber [16]		4.65	1.9	6.47 (*)
Granular activated carbon [16]		26.9	10.16	4.96 (*)
Cooled activated carbon(-60°C) [1, 5]		18.8 (*)	16.5 (*)	379 (*)

those of activated carbons, which have been used in underground experiments [11, 12]. Since the processed air was about $1 \text{ mBq}/\text{m}^3$ for 1 to 2 days after the Ag-zeolite columns were connected, it is considered to be sufficiently applicable to underground experiments through operational design such as parallelization of the zeolite columns and alternation of radon removal from the air and baking of the column.

6.2. Dependence of radon adsorption on humidity

3Ag-FER was measured for radon adsorption under two different humidity conditions in the carrier gas at refrigerator settings of -70°C and -90°C . The typical dew point temperatures of the carrier gas in the system during column bypass are -66°C and -86°C , respectively. As a result, as shown in Table 3, the value of K at the refrigerator setting of -70°C is about $1/4.5$ smaller than the value at -90°C . The decrease in radon adsorption capacity under high humidity environment was noted in previous studies by Ref. [8, 9], and this characteristic was also confirmed in this study. The typical dew point temperature of the carrier gas in the system after the zeolite column was connected was -92°C (see Appendix A). This indicates that using a carrier gas of lower dew point temperature than this should prevent moisture adsorption on the Ag-zeolite, and in that case, radon removal-only operation would be possible for a long period of time without baking.

6.3. Dependence of radon adsorption on silver content and silver introduction status

In this study, radon adsorption measurements were performed using Ag-zeolites with silver introductions adjusted to 3% and 8%. If the amount of silver is proportional to the amount of

radon adsorbed, then RT should vary in proportion to the amount of silver in this measurement system. Considering the actual amount of silver introduced in Table 2, and comparing the measurements at the refrigerator setting of -90°C in Table 3, 8Ag-FER-B and 3Ag-FER have a nearly proportional relationship between the amount of silver and the RT value. On the other hand, the value of RT for 8Ag-FER-D is considerably smaller than the value of RT expected from 3Ag-FER. Therefore, when introducing about 8% silver to FER, the "-B" method is better than "-D" method. Silver is introduced as metallic silver or silver ions, but due to the difference in the introduction method, the proportion of metallic silver is higher in "-D" than in "-B". This suggests that the most effective silver introduction for radon adsorption may be silver ions rather than metallic silver.

6.4. *Radon adsorption performance and application example for underground experiments*

In this study, 8Ag-FER-B showed the best radon adsorption properties in air, with a radon adsorption coefficient $K = 6506 \pm 81 \text{ m}^3/\text{kg}$. This is higher than the performance of Ag-zeolites to adsorb radon in air at room temperature tested in previous studies in Ref. [8, 9]. The granular activated carbon in Table 3 is equivalent to that used in the Super-Kamiokande radon removal system [4], and the cooled activated carbon is the actual performance in the Super-Kamiokande radon removal system. 8Ag-FER-B was found to have a higher radon adsorption coefficient than any of these adsorbents.

We now consider the application of 8Ag-FER-B to the Hyper-Kamiokande (HK) detector [17], the next generation of large underground water Cherenkov detector. The air purification system at HK is currently planing to produce dry air with a dew point temperature of -70°C at a flow rate of $54 \text{ Nm}^3/\text{hour}$ to supply the water purification system and the HK detector. The radon concentration in this dry air is expected to be about 50 Bq/m^3 , so radon must be reduced to $1/50000$ to achieve a radon concentration of 1 mBq/m^3 . The required retention time is $RT = 59.68$ days because radon will decay and decrease in the adsorbent while being adsorbed and retained. If the dew point temperature in the dry air can be reduced to -90°C by some pretreatment, about 12 kg of Ag-zeolite would be required in the case of 8Ag-FER-B to reduce the radon concentration in air to $1/50000$ at a flow rate of $54 \text{ Nm}^3/\text{hour}$. Even if two systems are constructed to operate in parallel for radon removal from the air and baking, the total weight would be 24 kg. In terms of volume, 24 kg of 8Ag-FER-B is about 35 L. The radon removal system in Super-Kamiokande [4] uses about 8 m^3 of room temperature activated carbon, and so on. Compared to this, it is likely that the system with Ag-zeolite can be made much smaller.

7. Conclusion

In this study, we focused on Ag-FER, which has been reported to have high performance against xenon in air, and measured its radon adsorption properties. The silver ion-exchanged zeolites used in these measurements were based on the zeolite from Tosoh Corporation, and silver ions were introduced into the zeolite by Sinanen Zeomic Co., Ltd. A dedicated measurement system was constructed at Kobe University, and five types of measurements were systematically performed using U-shaped columns of almost the same shape, yielding the following results.

As in the preceding studies, radon adsorption in air at room temperature was confirmed. The intrinsic radon emanation from 8Ag-FER-B was evaluated to be less than 45 mBq/kg (90% C.L.). This intrinsic radon emanation level is comparable to those of activated carbons, which have been used in underground experiments. In the case of 8Ag-FER-B, radon removal up to 1 mBq/m³ was observed for about 1 to 2 days after the start of the radon adsorption test, which indicates that 8Ag-FER-B can be applied to underground experiments. On the other hand, radon adsorption efficiency was found to be sensitive with respect to air humidity. In order to increase the efficiency of radon adsorption, dehumidification to a dew point temperature of about -86°C or lower is desirable. To increase the efficiency of radon adsorption, it was effective to increase the amount of silver. Furthermore, it was found that introducing silver in the form of silver ions, rather than metallic silver, is likely to be a good method to increase the efficiency of radon adsorption. The prototype of 8Ag-FER-B in this study showed higher radon adsorption performance than any of the preceding studies, and when 8Ag-FER-B is used in the Hyper-Kamiokande experiment, it is expected to be much smaller (12-24 kg) than the existing radon removal system using room-temperature activated carbon.

Acknowledgment

The authors would like to thank Kotaro Nagatsu (QST) and Jun Ichinose (QST) for their helpful discussions on radon removal performance of silver-ion exchanged zeolite from air. This work is supported by Japan Society for the Promotion of Science (JSPS) KAKENHI Grant Number 24H02243.

References

- [1] Y. Takeuchi et al., Phys. Lett. B, **452**, 418–424 (1999).
- [2] G. Pronost et al., Prog. Theor. Exp. Phys., **2018**, 093H01 (2018).
- [3] E. Aprile et al., Eur. Phys. J. C, **82**, 599 (2022).
- [4] Y. Fukuda et al., Nucl. Instrum. Meth. A, **501**, 418–462 (2003).
- [5] Y. Nakano, H. Sekiya, S. Tasaka, Y. Takeuchi, R. A. Wendell, M. Matsubara, and M. Nakahata, Nucl. Instrum. Meth. A, **867**, 108–114 (2017).
- [6] M. Murra et al., Eur. Phys. J. C, **82**, 1104 (2022).
- [7] M. Fukui et al., Xe adsorption performance of ag-loaded zeolite, In *The 36th Zeolite Research Presentation (on-line)*. The Zeolite Institute of Japan (2020).
- [8] S. Heinitz et al., Sci Rep, **13**, 6811 (2023).
- [9] O. Veselska et al., Prog. Theor. Exp. Phys., **2024**, 023C01 (2024).
- [10] K. Coopersmith et al., J. Phys. Chem. C, **127**, 1598–1606 (2023).
- [11] K. Abe et al., Nucl. Instrum. Meth. A, **661**, 50–57 (2012).
- [12] Y. Nakano et al., Prog. Theor. Exp. Phys., **2020**, 113H01 (2020).
- [13] H. Ogawa et al., JINST, **19**, P02004 (2024).
- [14] K. Hosokawa et al., J. Phys.: Conf. Ser., **469**, 012007 (2013).
- [15] K. Hosokawa, A. Murata, Y. Nakano, Y. Onishi, H. Sekiya, Y. Takeuchi, and S. Tasaka, Prog. Theor. Exp. Phys., **2015**, 033H01 (2015).
- [16] Y. Takagi, Measurement of radon removal performance of ambient temperature activated carbon in air for hyper-kamiokande (March 2024), Available at https://ppwww.phys.sci.kobe-u.ac.jp/seminar/pdf/Takagi_Mthesis.pdf.
- [17] K. Abe et al., Hyper-kamiokande design report (2018), arXiv:1805.04163.

A. Measured data

Here we present data on the measured radon concentration and dew point temperature changes.

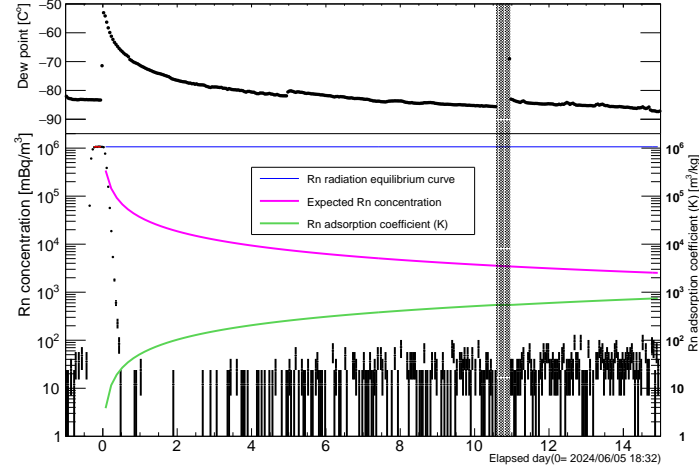


Fig. A1 8Ag-FER-B 44g, 1.57 SLM, -90°C (type and amount of Ag-zeolite, carrier gas flow rate, refrigerator temperature) measurement. Bottom panel: Variation of the radon concentration. Horizontal axis is elapsed day from the U-shaped column connection. The left (right) vertical axis is radon concentration in the radon detector (Rn adsorption coefficient). The red line shows the fitting result with the Rn source radiation equilibrium function. The blue line shows the extrapolation of the red line. Top panel: Variation of the dew point temperature. The horizontal axis is common with the bottom plot. The hatched area was not available to acquire data due to a planned power cut.

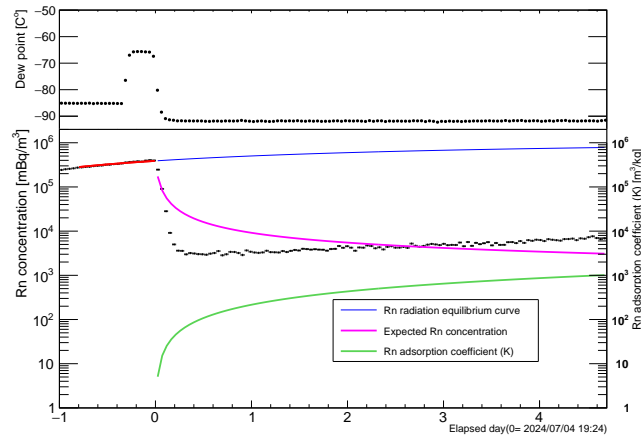


Fig. A2 3Ag-FER 20g, 3.00 SLM, -70°C measurement. Others are same as Fig. A1.

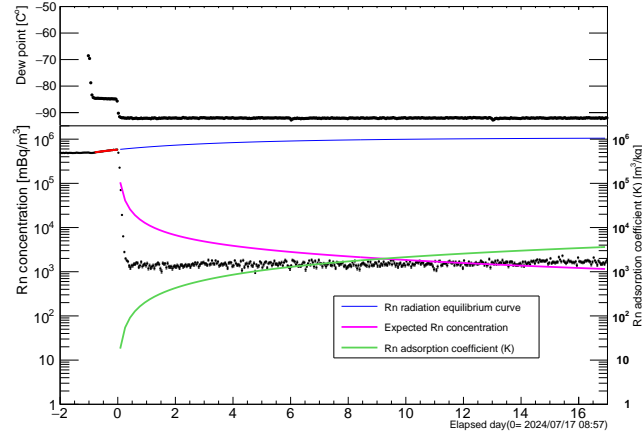


Fig. A3 3Ag-FER-B 20g, 3.00 SLM, -90°C measurement. Others are same as Fig. A1.

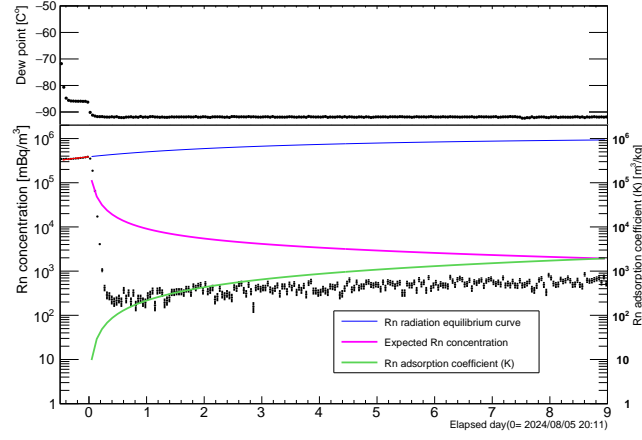


Fig. A4 8Ag-FER-B 20g, 3.00 SLM, -90°C measurement. Others are same as Fig. A1.

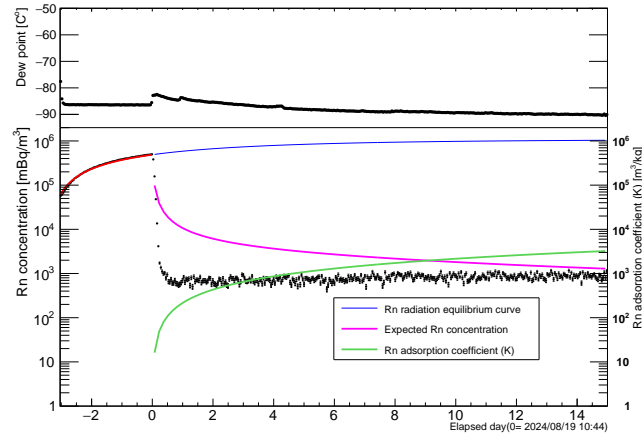


Fig. A5 8Ag-FER-D 20g, 3.00 SLM, -90°C measurement. Others are same as Fig. A1.